Rare Metal Materials and Engineering
Volume 49, Issue 8, August 2020
Available online at www.rmme.ac.cn

Science Press

Cite this article as: Rare Metal Materials and Engineering, 2020, 49(8): 2636-2643.

ARTICLE

Molecular Dynamic Simulations for Dissolution of Zn-Al Binary System

Yang Yao[1,2], Liang Yuxin[1,2], Li Shaorong[1], Li Bangsheng[1,2], Yan Jiuchun[1,2]

[1] State Key Laboratory of Advanced Welding and Joining, Harbin Institute of Technology, Harbin 150001, China; [2] School of Materials Science and Engineering, Harbin Institute of Technology, Harbin 150001, China

Abstract: Dissolution between zinc, aluminum and Zn-Al alloys are common in soldering, hot-dipping and coating, for example, when preparing Galvalumed steel and Galfan-coated steel products. For manufacturers, they need to ensure that Zn wet Al well in order to endow the prepainted material with excellent corrosion resistance. This work aims at finding some key factors which determine the degree of dissolution in different Zn/Al binary systems. The consideration of investigating kinetic factors in dissolutive wetting process is brought into molecular dynamic (MD) simulation. Different atomic scale wetting process are performed with LAMMPS, and simulation performances include Zn-5wt%Al, Zn-6.8wt%Al liquid models spreading on Al(100), Al(110), Al(111) solid substrates. By changing the temperature, elevating the percentage ratio of Zn and Al, it is found that Zn-Al binary dissolution can be pushed ahead by elevating temperature, or raising Al concentration in the liquid phase. The effects of temperature and atom percentages on dissolved volume and diffusion coefficient are also demonstrated by analyzing dissolutive parameters.

Key words: dissolution; molecular dynamics; contact angle; diffusion coefficient

Zinc-aluminum has long been a common alloy among coating materials, as an example, TC4 alloy shows desirable corrosion resistance characteristics after being coated by Zn-Al alloys[1]. Some workpieces of ships or bridge cables in use of galvanized steels are poor in sea-water corrosion resistance; however, if they could be coated by Zn-Al alloys, the corrosion resistance of steel sheets is better, compared with bare galvanized surfaces. Coated Zn-Al eutectic alloy endows the steel with both cathodic protection (by Zn) and oxidation protection (by Al).

The steel coated by 55 wt% Al-Zn was better known as Galvalume™, which was developed and commercialized first[2]. Zn-Al lamellar structure also prevented Galvalume coating steel from non-uniform corrosion behaviors. After that, Galfan™ was more frequently applied, owing to its corrosion resistance, superior mechanical and forming properties[3,4]. Galfan coating material was nominally Zn-5 wt%Al-mixed mischmetal alloy, and its component was near the binary eutectic point of Zn-Al. Adding 0.1%~0.3% RE could refine grains in Galfan coating structures, and thus would improve the corrosion resistance of steel wire.

A good wettability is essential for coating, hot-dipping, and soldering. Among all those metals, melting points of zinc, aluminum are relatively lower, so they are ideal solder materials. When processing Al workpieces, soldering the Al material with Zn or Zn-Al alloys is also practical, since they are active metals and have a good alloying ability. As indicated by ab-initio investigations, the electrode potential of Zn is close to that of Al[5]. Under such circumstance, dissolution process inside Zn-Al alloys is of great significance.

The research on solid phase's dissolution into liquid phase is commonly found. For the example, in Zn-Al binary liquid/solid metallic system, Zn and Al are both miscible metal elements, between which there is an unlimited mutual solubility. Wetting can be broadly classified into categories of non-reactive wetting and reactive wetting and the behavior of

Received date: August 10, 2019
Foundation item: National Natural Science Foundation of China (51435004)
Corresponding author: Yang Yao, Ph. D., State Key Laboratory of Advanced Welding and Joining, Harbin Institute of Technology, Harbin 150001, P. R. China, E-mail: hit1109103@163.com

substrate dissolution can be observed in reactive wetting process, so it is suitable to investigate dissolution phenomenon in some specific wetting systems[6,7]. Turlo[8] found that dissolution phenomenon played a central role in metals' reactive wetting process, because dissolution could produce heat for the reaction of liquid/solid phases[9]. Actually, mixing and phase transformation processes are activated together when dissolution happens, and dissolution kinetics is firstly controlled by diffusion, and further, by change of each phase's concentration. Such as in the system of Ni/Al, there is always a nanometric metallic multilayer, and dissolution is indicated to drive wetting system to alternate Ni, Al atoms in microstructure so as to form intermetallic compounds. All above point out that dissolution process can be coupled with dissolutive wetting, so the investigation of Zn-Al dissolution within binary Zn-Al wetting process is also reasonable.

Existing experimental methods are not accurate enough to investigate some sophisticated dissolution behaviors, and the solubility in micro diffusion is so hard to be analyzed[10]. Now numerical simulations have already been used to investigate some reactive processes, and molecular dynamics method suits for atomic scale diffusion, combination and mass transformation. Contact angle (CA) is an indicative parameter for solid/liquid interaction or dissolution. By contrast, CA can be observed better in MD simulation results of reactive wetting systems, such as Pb/Cu, Ag/Ni and Ag/Cu, and those CA values from simulations match well with those from experiments[11-13].

1 Experiment

Molecular dynamic simulations of Zn-Al dissolutive wetting were performed with massively parallel computers, equipped with highly efficient multiresolution algorithms. LAMMPS is a power tool for MD simulation. Besides, the appropriate potential function is a precondition for atomic dynamics calculations between Zn and Al phases. Here we used 2NN MEAM (2nd-neighbor modified embedded atoms) function to describe the interatomic potential between Zn-Zn, Zn-Al, Al-Al[14]. Parameters in 2NN MEAM are listed in Table 1, and each simulation lasted for 300 ps with 600 000 time steps. Nose-Hoover thermostat was used to monitor temperatures of atom groups in NVT. When activating dissolution, temperature should to be fixed; 380, 400 and 420 °C were set as simulation temperatures. Al(100), Al(110) and Al(111) facets were cleaved, used as substrates. Also, surface energies of Al facets at 380 °C were measured, through a cutting plane method.

During dissolutive wetting simulations, the atomic model must be placed in a finite slab; however, periodic boundary conditions were adopted for the solid atoms. Solid substrate is immensely vast, so it leaves enough space for liquid droplets to accomplish spreading and dissolving. The three liquid droplet models are namely Zn, Zn-11.3at%Al, and Zn-15at%Al, and the latter two are alloy models, so they need to be built with a Perl. Al(100), Al(110) and Al(111) facets were placed under hemispherical droplets; each consists of more than 20000 Al atoms. We finally left a 0.3 nm vacuum between each droplet and substrate.

Zn/Al(100), Zn/Al(111) and Zn/Al(110) atomic configurations are demonstrated by the screenshots in Fig.1. These substrate structures were all cleaved from Al fcc supercell, and the three facets are along [100], [110], [111] orientations, respectively. The diameters of droplet above are 6 nm and a Zn droplet is composed of 3000 Zn atoms. Droplet and substrate were merged in z direction. Afterwards, the construction was placed into one finite slab with 13.08 nm×12.90 nm×9.50 nm in size.

2 Results and Discussion

2.1 Temperature effects on Zn/Al dissolution

2.1.1 Zn/Al atomic structures after dissolutive wetting

MD simulation results of dissolutive wetting process show dynamic characteristics, and reveal the morphology of atomic structure. Some time-varied parameters like atom percentage, droplet volume and apparent contact angle (θ_A) can be measured. Besides, Al solid/vapor surface energy (γ_{sv}) computational results are different. γ_{sv} of Al(110), Al(100) and Al(111) planes are 0.903, 0.860 and 0.753 J/m^2 at 380 °C, respectively, indicating γ_{sv} of Al(110) is larger. Al planar density and the surface energy are directly related[15]. Viewing the cross-section snapshots of droplet/substrate structures in Fig.2, wetting characteristics of three Zn/Al systems in equilibrium states are different. When θ_A values are stable, Zn/Al(111), Zn/Al(100) are partly mixed, while the substrate of Zn/Al(110) becomes totally distorted. The planar density is determined by dissolution in substrate. (110) plane's density is 0.86 atom/nm, which is the smallest, so Zn-Al dissolution brings the most significant changes to Al(110) substrate structure. By contrast, the planar densities of Al(100) and Al(111) are 1.22 and 1.41 atom/nm, respectively, which are slightly minor.

Table 1 Zn-Al MEAM potential

Phase	E_c/eV	L/nm	a/nm	A/eV	$t_{(1)}$	$t_{(2)}$	$t_{(3)}$	Attrac	Replus	R_{cut}/nm
Zn	1.3	0.28	0.7	0.7	25	−17	51.5	0.1	0.1	0.7
Al	3.4	0.41	0.47	1.2	3.1	0.5	7.75	0	0.1	1
Zn-Al phase	2.8	0.29	0.46	-	-	-	-	0.08	0.075	0.71

* E_c is cohesive energy per atom when at equilibrium states; L and a are constant parameters of each lattice; in MEAM, A is a specialized parameter, while $t_{(1)}$, $t_{(2)}$, $t_{(3)}$ are three dimensionless standard parameters; R_{cut} is the cutoff distance set artificially; in this table, additional attraction Rose energy terms are Attrac(i, j), Replus(i, j), and their values are set between 0 and 1

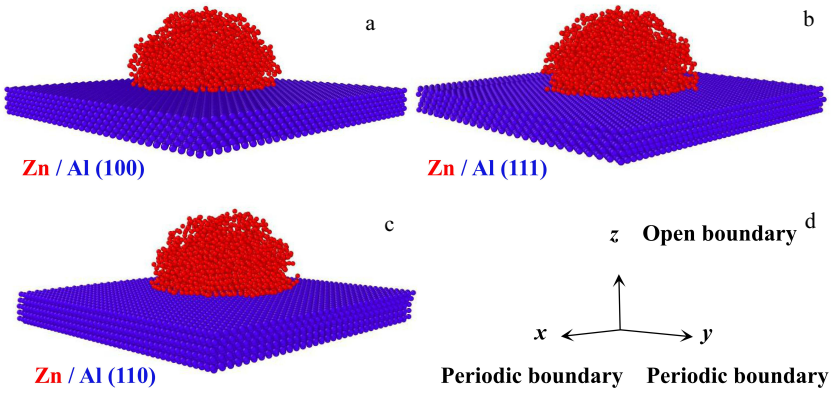

Fig.1 Zn droplet on Al(100) substrate (a), Al(111) substrate (b), and Al(110) substrate (c); (d) the boundary condition

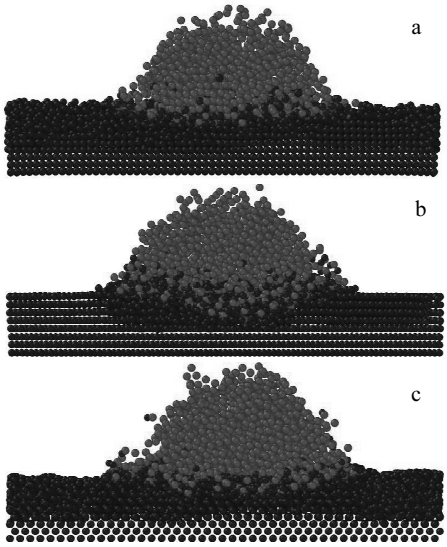

Fig.2 Cross-section screenshots of Zn/Al wetting structures at 380 °C after 300 ps: (a) Zn/Al(100), (b) Zn/Al(111), and (c) Zn/Al(110)

Table 2 lists θ_A results in dissolutive wetting simulations, with ambient temperatures 380, 400, 420 °C. By analyzing θ_A and the planar density, apparent contact angle is influenced by planar density, θ_A on Al(110) are the largest when at the same temperature, so wettabilities of Zn/Al(100) and Zn/Al(111) are always better than that of Zn/Al(110).

Density profiles were here used to demonstrate change in the atomic percentage. According to Table 2, the Zn/Al(100) system has a lower θ_A, therefore we have depicted ultimate density profiles for Zn/Al(100) structures, as shown in Fig.3. In those density profiles, the Zn/Al saturates at three different percentages, so they are used for calculating atomic densities at 380, 400 and 420 °C. For calculating Al, Zn dissolved contents, the distortional zone around the solid-liquid interface was divided into 20 parallel layers. The primitive solid-liquid

Table 2 Apparent contact angles and Al planar densities in Zn/Al dissolutive wetting simulations

Temperature/°C	Surface	Planar density of Al substrate/atom·nm^{-1}	Zn apparent contact angle/(°)
380	Al(100)	1.22	50.2
	Al(110)	0.86	52.1
	Al(111)	1.41	51.6
400	Al(100)	1.22	45.6
	Al(110)	0.86	50.5
	Al(111)	1.41	48.8
420	Al(100)	1.22	39.1
	Al(110)	0.86	47.5
	Al(111)	1.41	46.3

interface has been illustrated in Fig.3d, which locates in the middle region, so the point is marked as z=0 nm. The slab model was then segmented into pieces every 0.2 nm in height till up to the bottom plane of the substrate (−2 nm). A Zn-Al compound area is shown near the 0 nm district, as the main district where Zn and Al atoms mix in.

Density profiles can show the distribution of two elements, where we find the existence of an atomic layer with 50% Zn atoms and 50% Al atoms above the primitive interface. After the simulation, there are more Al atoms in the droplet, but less number of Zn atoms dissolving towards Al substrate. This difference in solubility results from thermal properties of Zn and Al. Since the melting point of Al is higher than that of Zn, there is not enough energy to destroy connections among Al atom groups in simulation and Zn atoms would not path into Al lattice structures. Meanwhile, Al atoms have larger potentials to dissolve into liquid Zn structure passing through Zn-Al interface.

According to atomic kinetic theories, elevating wetting temperature affects atomic inter-diffusion positively, but the promotion degree can be different. A higher temperature promotes atoms' mobility step further which breaks the balance of binary interdiffusion. After elevating wetting temperature, the diffusivity of Al is greater than that of Zn; therefore, temperature

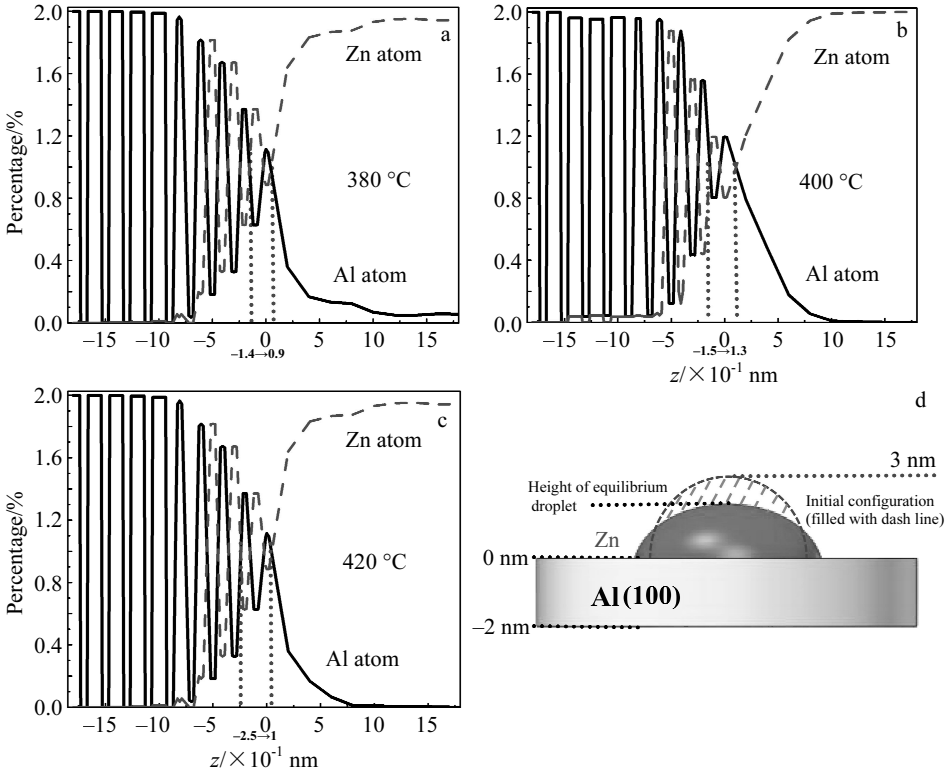

Fig.3 Density profile charts of Zn/Al(100) wetting at different temperatures: (a) 380 °C, (b) 400 °C, (c) 420 °C; (d) a dynamic wetting diagram with the designation of vertical height

elevation enhances interdiffusion as well as wettability, so the degree of dissolution in Zn/Al wetting is also temperature related. Dissolution enlarges the depth of Zn-Al compound layer when temperature changes from 380 °C to 420 °C. We compared the thickness of layers at the three different temperatures. The thickness shows a peak value of 0.35 nm under the condition that dissolution is activated at 420 °C. At 400 °C, the region of Zn-Al compound becomes smaller, and its thickness reduces to 0.28 nm. Similarly, it gets even thinner if temperature is brought down to 380 °C, which has a thickness of 0.23 nm.

2.1.2 Dissolved contents in Zn/Al wetting

Lower angle (θ_B) characterizes the degree of dissolution in wetting, which is related to the kinetic formation of dissolution pit. In Fig.4, we symbolize the dissolution degree with the size of spherical cap. We find θ_B serves as an instruction for dissolved content, and θ_B value is on an increasing trend with the temperature rise.

Supposing the volume of an undissolved part of liquid is V_A, while V_B accounts for the volume of a dissolved part inside, Eq. (1) describes a function,

$$V_B = \left[V_A \cdot f(\theta_B)\right] / f(\theta_A) \quad (1)$$

using which V_B, V_A can be related together through estimating $f(\theta_i)$ (i=A, B) function values. Yost provided a formula for the calculation of $f(\theta_i)$, which has the expression as Eq. (2)[9].

$$f(\theta_i) = \frac{2+\cos\theta_i}{1+\cos\theta_i}\sqrt{\frac{1-\cos\theta_i}{1+\cos\theta_i}} \quad (2)$$

Wetting configurations inside Fig.4b~4d can all demonstrate equilibrium atomic structures of Zn-Al. Values of θ_A, θ_B, the calculated V_A and V_B are all available with those screenshots. By comparison, apparent contact angle has a positive correlation with temperature, and θ_B value also shows a proportional relationship with the wetting temperature. The dissolved content V_B demonstrates the tendency of Zn phase dissolved in Al substrate. In the last chapter, the temperature effects on Zn/Al wettability has been proved through the comparison of θ_A. If Zn/Al system gets a well wettability, most kinetic energy of Zn atoms will be consumed in the spreading process, while only the rest can be used to promote the potential energy of Zn-Al system. However, temperature promotion happens to supply more energy for Zn atoms in the solid phase, which explains why θ_B is forced to increase at a higher wetting temperature. While the correlation between temperature and V_B is not distinct, there are not distinctions between degrees of Zn-Al dissolution at 400 and 420 °C.

2.2 Effect of Al concentration on Zn-Al/Al dissolution

2.2.1 Dissolutive parameters in Zn-Al/Al wetting

In the MD wetting process, the variation of solder's Al concentration affects the equilibrium atomic structure, as well

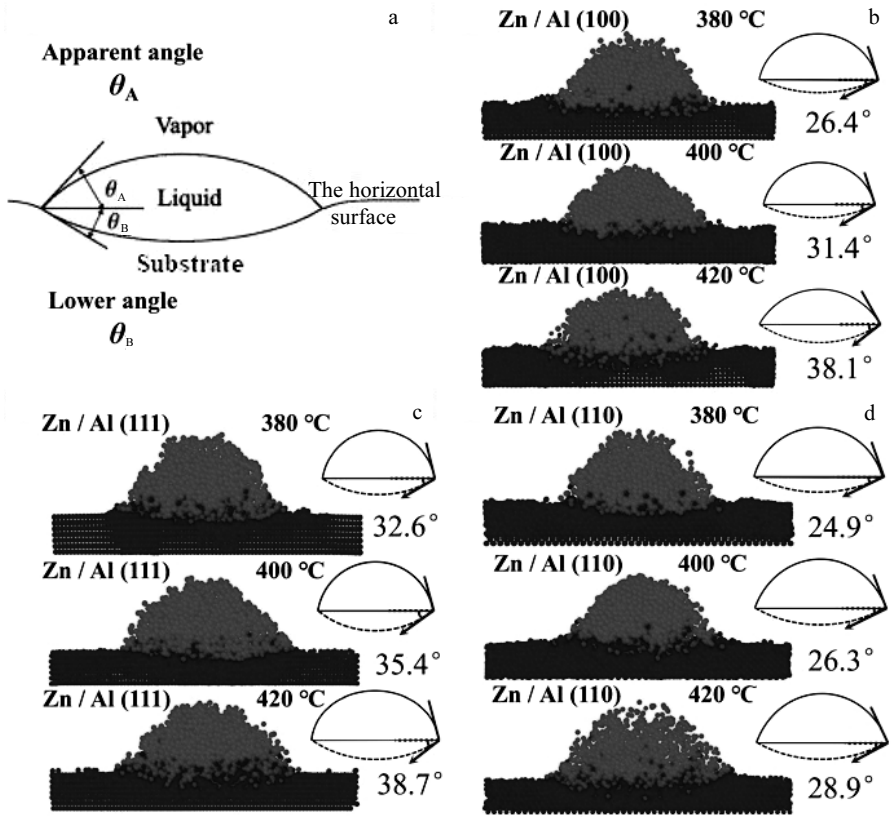

Fig.4 An instruction for θ_A, θ_B measurements (a); dissolutive wetting configurations of Zn/Al(100) (b), Zn/ Al(111) (c), and Zn/Al(110) (d)

as the melting temperature of liquid phase. Those effects can be definitely embodied in Zn/Al dissolution process, during the simulation of dissolutive wetting. Parameters were measured with three simulation series, and apparent contact angles, lower angles at 380, 400, and 420 °C were recorded as shown in Table 3.

By comparison, the apparent contact angle decreases when Al atomic concentration is increased. Temperature indeed improves Zn/Al wettability in Zn-Al/Al systems; at the same time, a higher Al concentration also enhances the Zn/Al system's wettability to some extent. By surface thermodynamic theories, the Young's equation (3) includes liquid-vapor, solid-vapor, and solid-liquid surface energies marked as γ_{lv}, γ_{sv} and γ_{sl}. So adding more Al definitely narrows the gap between γ_{lv} (Zn) and γ_{sv}. When wetting process reaches equilibrium, the γ_{lv} decreasement by elevating Al's concentration in Zn-Al will cut down the value of θ_A, and thus the wettability is improved.

$$\gamma_{lv}\cdot\cos\theta_A = \gamma_{sv}-\gamma_{sl} \quad (3)$$

Dissolution degrees are demonstrated with twenty-seven θ_B values. Roughly speaking, if more Al distributes in liquid phase, the limitation of Zn-Al dissolution becomes weaker so Zn-Al/Al spreading tendency gets enhanced. In the same Zn-Al binary system, spreading and dissolution parallel activates; the more heavily θ_A reduces, the larger extent θ_B decreases in. And according to Table 3, among groups of Zn/Al, Zn-15at%Al/Al and Zn-11.3at%Al/Al, the trend of θ_B values is upwards.

Table 3 Dissolutive parameters of all wetting simulations for Zn-*x*at% Al (*x*=0, 11.3, 15)

Temperature/°C	Surface	*x*=0	*x*=11.3	*x*=15
380	(100)	θ_A=50.2°	θ_A=48.1°	θ_A=45.5°
		θ_B=16.2°	θ_B=15.3°	θ_B=14.2°
	(110)	θ_A=52.9°	θ_A=52.1°	θ_A=51.0°
		θ_B=8.8°	θ_B=9.6°	θ_B=10.4°
	(111)	θ_A=51.6°	θ_A=51.1°	θ_A=50.0°
		θ_B=17.6°	θ_B=17.3°	θ_B=16.7°
400	(100)	θ_A=45.6°	θ_A=46.5°	θ_A=43.7°
		θ_B=26.3°	θ_B=25.9°	θ_B=23.1°
	(110)	θ_A=50.5°	θ_A=49.5°	θ_A=49.0°
		θ_B=14.7°	θ_B=15.8°	θ_B=16.2°
	(111)	θ_A=48.8°	θ_A=49.3°	θ_A=39.9°
		θ_B=33.0°	θ_B=31.2°	θ_B=23.7°
420	(100)	θ_A=39.1°	θ_A=38.2°	θ_A=37.4°
		θ_B=28.2°	θ_B=24.2°	θ_B=21.9°
	(110)	θ_A=47.5°	θ_A=43.2°	θ_A=39.5°
		θ_B=16.7°	θ_B=17.5°	θ_B=18.2°
	(111)	θ_A=46.3°	θ_A=42.9°	θ_B=41.9°
		θ_B=36.5°	θ_B=29.8°	θ_B=26.3°

Relationships between Zn-Al dissolution and Al concen-

tration can be verified after the calculations of dissolved volumes. Fig.5 illustrates how the dissolved volume V_B varies within different dissolutive wetting groups, including Zn (liquid)/Al (solid) and Zn-Al (liquid droplets)/Al (solid substrates). The ratio V_B/V_A demonstrates that how much of droplet's volume has dissolved into Al(100), Al(110) and Al(111) substrates after finishing dissolutive wetting.

Compared with the dissolved volume of Zn/Al system, Zn-Al dissolution gets promotion in wetting systems which include Zn-11.3 at%Al and Zn-15 at%Al alloy droplets. The rule can be applied to Zn-Al solders. In the process of dissolving into several substrate models, Al(100), Al(110) and Al(111) have been used during the whole series of MD simulation. Dissolution enhancement is even more significant with a high wetting temperature. In Fig.5a~5c, the increasing trend of solubility is rendered quite slow. In 380 °C dissolutive wetting, a smooth curve appears (lines in black), demonstrating the steady V_B/V_A ratio, but the curve's slope at 400 and 420 °C are larger than that at 380 °C. By comparison, we find change of solubility becomes more significant at high temperatures. With the premise that spreading can progress fast by raising the system's temperature but longer time must be needed, we achieve to explain why V_B decreases at higher temperatures. At higher temperatures, the effects of Al concentration on Zn-Al/Al dissolution are more significant.

2.2.2 Diffusion coefficient of Zn-Al/Al

Coefficient D is a key parameter of mass transportation, revealing the diffusivity of atoms in liquid-solid phases. If a wetting system has high capacity of transporting atoms, a larger D should appear in its dissolution process. With the cumulative degree of atomic displacement, the diffusion coefficient value is related to atoms' mean square displacement (MSD). The mean variance can be estimated by instantaneous atomic coordinates as Eq.(4) has shown.

$$\mathrm{MSD}(t)=\frac{1}{n}\sum_{i=1}^{n}\left\langle\left|r_n(t)-r_n(0)\right|^2\right\rangle \quad (4)$$

where, $r_n(t)$ and $r_n(0)$ are namely displacement vectors at time t and initial moment t=0, respectively, with n atoms in a group. The calculation of diffusion coefficient D obeys Einstein diffusion equation. In Eq. (5), the relationship between D-t is established. The interactive effect of temperature and the Al content on Zn-Al dissolution also relies on phase transformation behavior at different temperatures. Among the selected temperature range 380~420 °C, the Zn-Al liquidus temperature line corresponds to Zn atom percentage of 80%~88.7%.

$$D = 1/6\lim<\mathrm{d}|r_n(t)-r_n(0)|^2/\mathrm{d}t> \quad (5)$$

In Fig.6, twenty-seven measured D values are divided into three groups on the basis of substrate structures. In Zn-Al/Al(100), Zn-Al/Al(110) and Zn-Al/Al(111) groups, the change of diffusion coefficient value depends on the concentration of Al within droplet phases.

Fig.7 is the Zn-Al phase diagram, and formation temperature of Zn-11.3at%Al is nearly 380 °C, while Zn-15at%Al alloy's forming temperature is 400 °C. Fig.7 also indicates that Zn-Al is a typical binary eutectic alloy, while Zn-11.3at%Al, Zn-15at%Al belongs to Zn-Al eutectic alloy and Zn-Al hypereutectic alloy, respectively.

It is indicated that when solid Al is diffused by Zn-11.3at%Al, the speed of dissolution is slower, rather than

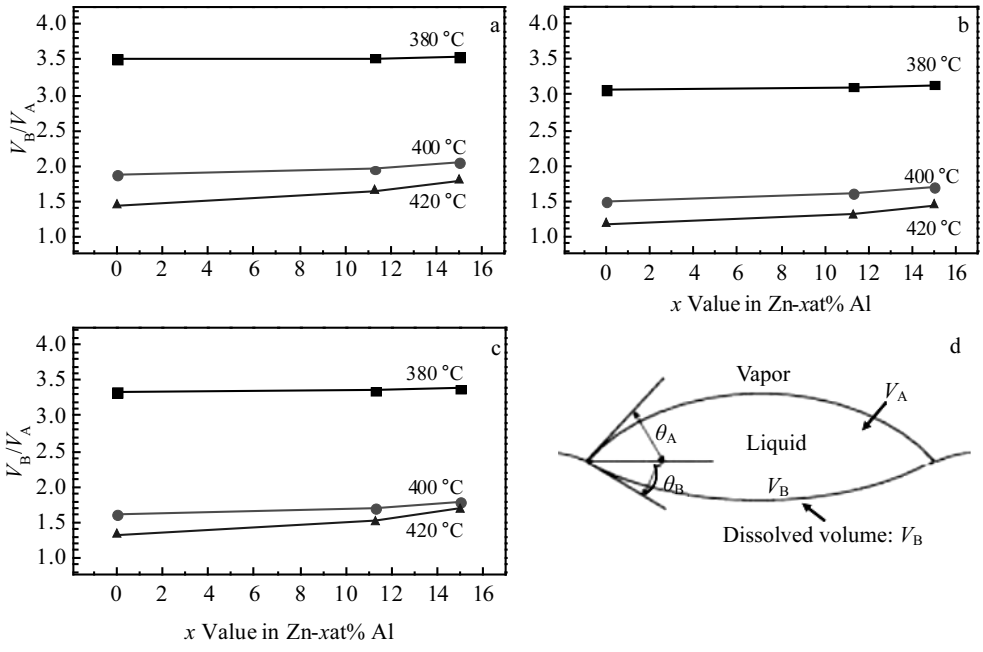

Fig.5 V_B/V_A ratios of Zn/Al(100) (a), Zn/Al(110) (b), Zn/Al(111) (c); (d) schematic diagram for calculating V_A, V_B

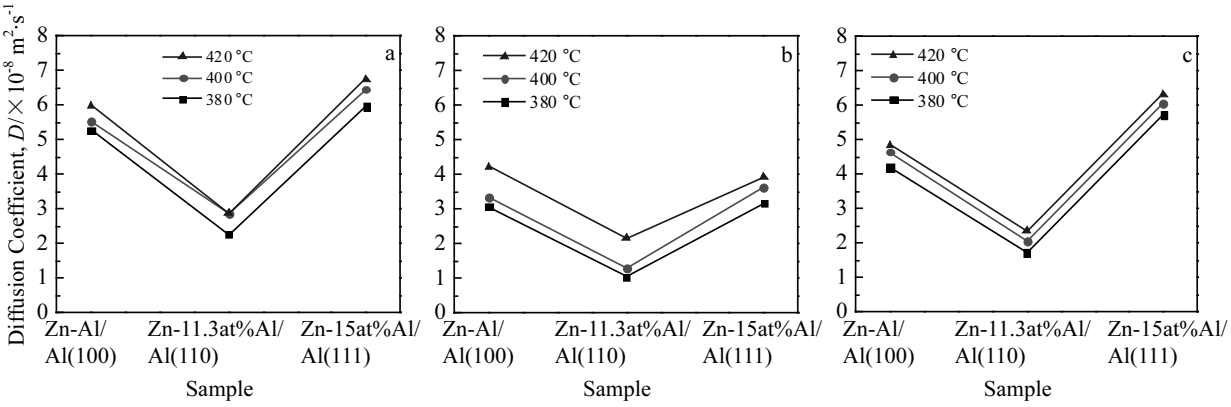

Fig.6 Diffusion coefficients in Zn-Al/Al(100) (a), Zn-Al/Al(110) (b), and Zn-Al/Al(111) (c) wetting

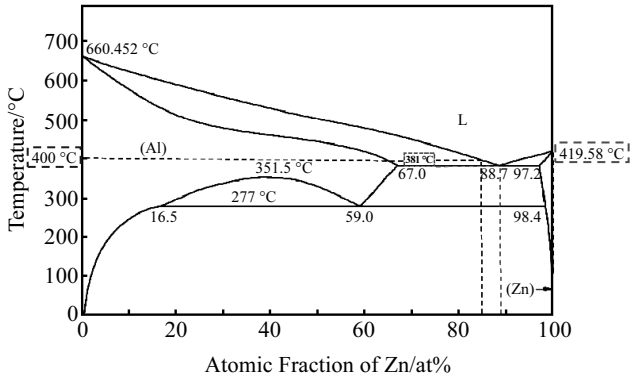

Fig.7 Zn-Al phase diagram

being diffused by pure Zn. From the Zn-Al phase diagram, 88.7/11.3 is the exact eutectic point for their alloying, so combining and alloying happen to slow down the progress of Zn-Al dissolution. Meanwhile, when diffused by Zn-15at%Al, the diffusion coefficient rises, which means that the dissolution is getting faster. We conclude that hypereutectic Zn-Al alloy has larger solubility than eutectic Zn-Al alloy on the basis of the Zn-Al simulation and their phase diagram. The MEAM potential we used for Zn-Al is appropriate to describe the pair function between Zn-Zn, Al-Al and Zn-Al atom groups, so it predicts the melting point and solubility well for Zn-Al alloy[16].

3 Conclusions

1) We investigated the contact angle, lower contact angle and dissolved content in Zn-Al/Al(100) wetting systems at 380, 400, 420 °C. At 420 °C, the wetting dynamic process shows the smallest apparent contact angle, being 37.4°. Lower angle is affected by the interaction of temperature and Al content. Dissolved volume of droplet increases when Al content in the two-component Zn-Al alloy droplet increases.

2) Zn/Al wetting parameters are deeply related to the solubility of Zn-Al dissolution. Both temperature's elevation and the droplet's Al addition have positive effects on Zn-Al dissolution.

3) Diffusion coefficient indicates that the diffusivity of atoms is elevated when Al concentration in liquid phase increases. The largest level of Zn-Al interdiffusion appears when Zn-15 at% Al dissolves into an Al(100) substrate at 420 °C.

References

1 Liu X B, Barbero E, Xu J *et al. Metallurgical and Materials Transactions A*[J], 2005, 36: 2049
2 Khezrloo A, Derabi F E, Tayebi M *et al. Silicon*[J], 2018, 10: 2431
3 Wang R N, Zhang P Z, Wang Y F *et al. Materials and Corrosion*[J], 2014, 65(9): 913
4 Zhang X, Wallinder I O, Leygraf C. *Surface Engineering*[J], 2018, 34(9): 641
5 Zhao M, Zhou M, Jiang Q. *Journal of Materials Science Letters* [J], 1998, 17: 2079
6 Moon J, Lowekamp J, Wynblatt P *et al. Surface Science*[J], 2001, 488(1-2): 73
7 Cherukara M J, Weihs T P, Strachan A. *Acta Materialia*[J], 2015, 96: 1
8 Turlo V, Politano O, Baras F. *Journal of Applied Physics*[J], 2017, 121(5): 055 304
9 Yost F G, Sackinger P A, O'Toole E J. *Acta Materialia*[J], 1998, 46(7): 2329
10 Xia Y, Steen P H, Richet N *et al. Journal of Mathematical Fluid Mechanics*[J], 2018, 841: 767
11 Timoshenko V, Bochenkov V, Traskine V *et al. Journal of Materials Engineering and Performance*[J], 2012, 21: 575
12 Benhassine M, Saiz E, Tomsia A P *et al. Acta Materialia*[J], 2010, 58(6): 2068
13 Webb III E B, Grest G S, Heine D R *et al. Acta Materialia*[J], 2005, 53(11): 3163
14 Jang H S, Kim K M, Lee B J *et al. Calphad*[J], 2018, 60: 200

15 Chen S D, Soh A K, Ke F J. *Scripta Materialia*[J], 2005, 52(11): 1135

16 Dickel D E, Baskes M I, Aslam I *et al*. *Modelling and Simulation in Materials Science and Engineering*[J], 2018, 26: 045 010

锌/铝二元体系中溶解现象的分子动力学模拟

杨 尧[1,2]，梁玉鑫[1,2]，李绍荣[1]，李邦盛[1,2]，闫久春[1,2]

(1. 哈尔滨工业大学 先进焊接与连接国家重点实验室，黑龙江 哈尔滨 150001)

(2. 哈尔滨工业大学 材料科学与工程学院，黑龙江 哈尔滨 150001)

摘 要：锌，铝和锌铝合金之间的溶解作用常见于钎焊，热浸镀和涂覆过程，如制备 Galfan、Galvalume 镀层钢的过程。工件如要通过预制的涂层获得良好的抗腐蚀性能，需使镀层材料中的锌和铝之间有良好的润湿，本工作探究在不同的 Zn-Al 二元合金体系中，影响锌和铝溶解程度的几个关键因素，将动力学影响因素融入分子动力学模拟当中。原子尺度下的溶解润湿现象通过 LAMMPS 来模拟，其中包含了 Zn-5wt%Al (Zn-11.3at%Al)和 Zn-6.8wt%Al (Zn-15at%Al)合金在 Al 的(100)，(110)和 Al(111)表面的润湿模型。通过改变温度，提升 Zn，Al 之间的原子分数比，发现升高温度，提高液相中的 Al 含量可以促进 Zn-Al 组元的溶解。同时，本工作也通过分析表征溶解参数的变化，研究了温度、Al 含量对溶解部分体积和扩散系数大小的影响。

关键词：溶解；分子动力学；接触角；扩散系数

作者简介：杨 尧，男，1993 年生，博士，哈尔滨工业大学先进焊接与连接国家重点实验室，黑龙江 哈尔滨 150001，E-mail: hit1109103@163.com